International Journal of Material Forming (2023) 16:39
https://doi.org/10.1007/s12289-023-01758-z

ORIGINAL RESEARCH

Advanced direct extrusion process with real-time controllable extrusion parameters for microstructure optimization of magnesium alloys

Leire Elorza Azpiazu[1,2] · Aritz Egea[1] · Dietmar Letzig[2] · Changwan Ha[2,3]

Received: 4 November 2022 / Accepted: 2 May 2023 / Published online: 7 June 2023

Abstract
The extrusion speed and deformation temperature are important factors affecting the microstructure development during the deformation. Microstructure development plays a crucial role in the performance of the mechanical properties of materials. In direct extrusion, the homogeneous evolution of the microstructure in the length of the extruded bar could be affected due to its non-isothermal exit temperature evolution. Thus, a new set-up is suggested with real-time controllable speed and temperature to characterize the influence of temperature on the microstructure and obtain its homogeneous development for the magnesium alloy. During the extrusion, the temperature of the extruded bar is evaluated by using the infra-red camera, and the extrusion speed is simultaneously controlled in real-time depending on the temperature difference between a set temperature reference and the one obtained from the infra-red camera. This suggested set-up of extrusion is evaluated in terms of the microstructure and temperature evolution of the extruded bar.

Keywords Processing control · Isothermal extrusion · Microstructure control · Infra-red camera · Magnesium alloy

Introduction

The global requirement for energy efficiency improvement and greenhouse gas emission reduction has prompted automotive and aerospace industries to consider weight-saving materials. Under these circumstances, wrought magnesium alloys receive attention as an option to achieve lightweight products with good mechanical properties [1]. The forming processing of Mg alloy is generally used at elevated temperatures ranging from 300 to 450 °C [2]. The homogeneity of microstructure in Mg alloys is an important factor determining the material properties during the general forming, e.g. extrusion and rolling, at elevated temperatures for industrial application. It is exhibited that the temperature of the extruded profile is increased during the deformation due to internal friction between the billet, container wall, and die, resulting in a non-isothermal process, especially in direct extrusion. The increasing temperature enhances dynamic recrystallization (DRX) and static recrystallization (SRX), which can result in the inhomogeneous microstructure of the material [3]. Isakovic et al. [4], for example, have shown a grain coarsening effect in the length of directly extruded 3Al-1Zn (AZ31) magnesium alloy due to the temperature gradient of the bar. The inhomogeneous microstructure can negatively impact the mechanical properties [5]. Thus, producing a homogeneous microstructure in the forming process is essential.

During the extrusion process, recrystallization could be controlled by reducing the temperature resulting from implementing an immediate force cooling in the die exit of the extrusion. Different cooling methods, e.g. air [6] and sprayed water cooling [7–9], have refined the grain due to DRX restriction by effective temperature reduction. However, forced cooling methods have not obtained an isothermal extrusion, and the microstructure's homogeneity has yet to be reported.

✉ Leire Elorza Azpiazu
lelorza@mondragon.edu

✉ Changwan Ha
changwanha@postech.ac.kr

1 Faculty of Engineering, Mondragon Unibertsitatea, 20500 Arrasate-Mondragón, Spain

2 Institute of Material and Process Design, Helmholtz-Zentrum Hereon, D-21502 Geesthacht, Germany

3 Present Address: Beamline Engineering Team, Pohang Accelerator Laboratory, POSTECH, Pohang, Republic of Korea

The extrusion speed also affects the microstructure's uniformity [4, 5]. High extrusion speed enhances the internal friction, increasing the temperature on the extruded bar. It has been reported that the low extrusion speed achieves grain refinement during the extrusion of AZ31 alloys [5, 10–12]. Moreover, different extrusion speeds have developed different microstructures of the extruded profile. Indeed, the control of the extrusion speed can play a similar effect with the temperature control on the microstructure development during the extrusion.

Several works have reported that variable speed extrusion can result in a constant exit temperature of the bar. Chanda et al. [13] have probed by the finite element method (FEM) simulations that an isothermal extrusion with homogeneous microstructure could be obtained by varying the extrusion speed. In [14–16], isothermal extrusions have been developed with predetermined ram speed profiles. FEM simulations and the Proportional, Integral, and Derivative (PID) control algorithms have been used to obtain the mentioned speed profiles [15, 16]. Nevertheless, the main drawback of these methods is that a new speed profile should be obtained for different extrusion parameters (initial billet temperature, billet geometry, ambient temperature), or a specific temperature at the exit is desired. This leads to high computational requirements. Moreover, the microstructure evolution obtained during isothermal extrusion was not analyzed.

Considering the mentioned disadvantages, this study suggests extrusion speed control in real-time to achieve the homogeneous microstructure of Mg-AZ31 alloy. During the extrusion, the temperature and speed are controlled in real-time using the infra-red camera (IRCAM) and OPC (Open Protocol Communication) communication protocol. Based on the temperature control, the tracked temperature is consistently retained with the controlled extrusion speed. In such a manner, preliminary FEM simulations could be avoided. The obtained results are discussed on the temperature and microstructure evolution of the AZ31 alloy in different extrusion conditions.

Experimental procedure and set-up

AZ31 magnesium alloy (Mg - 3.1 Al - 0.68 Zn, in wt.%) was gravity cast to produce billets for extrusion, which was machined to a diameter of 49 mm and a length of 150 mm. The billet was homogenized at 400 °C for 16 hours and quenched in water. Direct extrusion was conducted at 300 °C as a round bar with a diameter of 8 mm, which corresponds to an extrusion ratio of 1:37.5. The extrusion speed was set at 5 mm s^{-1}, 0.5 mm s^{-1} (named as E5 and E05, respectively), and controlled multi-speed between 0.1-1 mm s^{-1} (named as EMS). A horizontal construction extrusion press from Müller Engineering with a maximum press capacity

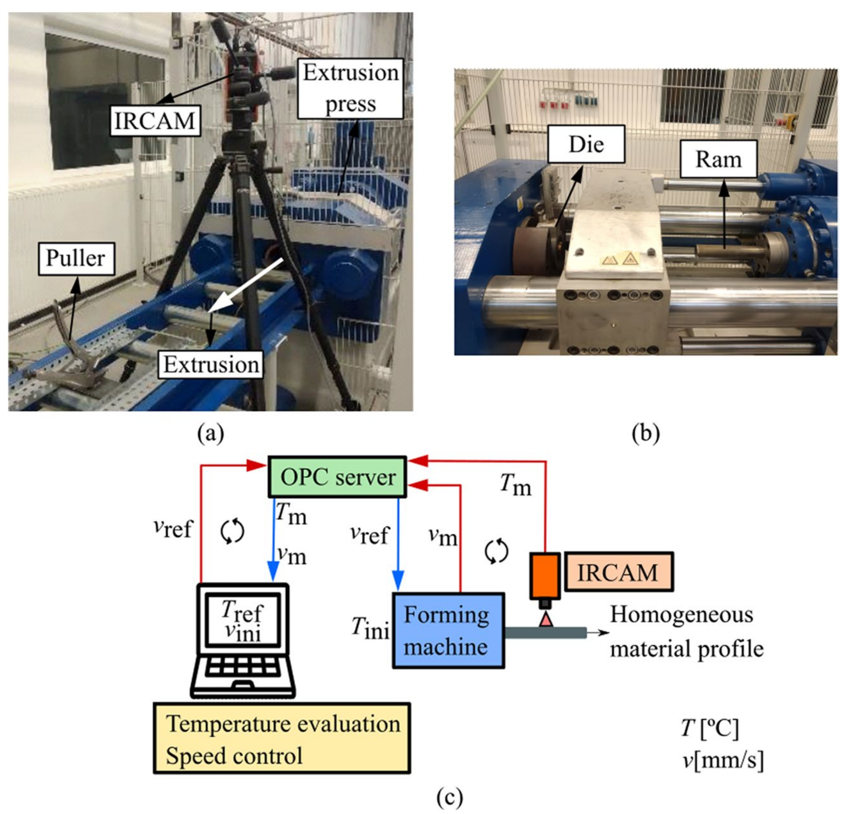

Fig. 1 **a** Direct extrusion set-up with extrusion press, puller and IRCAM; **b** Extrusion press die and ram; **c** advanced controllable speed and temperature extrusion system scheme (T_{ref}: reference temperature, v_m: measured speed, T_m: measured temperature, T_{ini}: initial temperature, v_{ini}: initial speed)

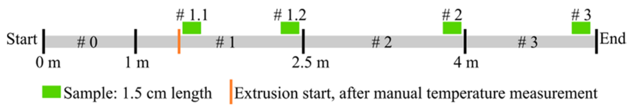

Fig. 2 Schematic representation of sample position for microstructure observation in different sections of the extruded bar

of 2.5 MN was used (Fig. 1a and b). To ensure extrusion stability, the billet, container, and ram were preheated to extrusion temperature (300 °C) prior to the extrusion. An IRCAM (VELOX 327 k SM) was installed at the die exit to measure and track the temperature of the extruded bar. The temperature was manually measured by a thermocouple at the beginning and end of the extrusion so that the temperature measured from the IRCAM was calibrated in the software. The schematic set-up installed at the extruder is depicted in Fig. 1a.

Figure 1c shows the scheme of the advanced extrusion system with controllable speed and temperature used in the EMS. The desired temperature for the extruded material profile (T_{ref}) was obtained with the adjustment of the extrusion speed (v_{ref}), depending on the difference (error) between the reference and measured (T_{m}) temperatures. The control system was employed in real-time until the end of the extrusion. The control system has four main elements: the forming machine (extrusion press), the IRCAM (for measuring the temperature), the communication protocol based on the OPC connection system (for data exchange), and the temperature evaluation and speed control (implemented in the PC).

For microstructure observation, the extruded sample was measured using the optical microscopy after the sample preparation by mechanical polishing and etchant techniques on longitudinal sections of the extruded bar. The average grain size was determined by using computer-assisted linear intercept measurements at different sections for the whole extruded bar, as shown in Fig. 2.

Results and discussion

Live speed control system validation

To ensure the proper control of the temperature and speed, it was necessary to have a real-time accurate temperature acquisition and evaluation using the IRCAM. Figure 3a and b represent the results obtained by implementing real-time temperature acquisition and evaluation. Figure 3a compares manual and live evaluations for the temperature measurement during the extrusion. It can be observed that the live evaluation appropriately works to collect the average temperature at the extruded bar in real-time without delay. However, when an unfocused image is captured (Fig. 4a), due to the bar oscillations derived from high extrusion speed, the IRCAM cannot get the correct temperature of the bar. The unfocused images cause incorrect data measurement and abrupt temperature decreases (Fig. 3a, marked as a dashed line), causing temperature reading issues. Therefore, the unfocused images are discarded based on the number of pixels of the bar, as the obtained bar has a constant cross-section. If the number of data between the bar edges in the current image is higher than the previous images (Fig. 4b), the current image is not used to evaluate the temperature. Figure 3b compares the manual evaluation, live evaluation (without discarding the unfocused images) and live evaluation improved (discarding unfocused images). It can be observed that the live evaluation improved curve appropriately reproduced the manual evaluation. Therefore, the implemented live temperature evaluation system can correctly perform the temperature acquisition during the extrusion if unfocused images are not considered.

In addition, a simple temperature-dependent speed control is implemented to validate the system. This speed control is developed based on a lookup table. A speed reference between 0.1 and 1 mm s^{-1} is set depending on the error between the reference and measured temperatures. Generally, the predefined ram speed applied in previous

Fig. 3 Comparison of temperature (**a**) manual and live evaluation; **b** manual, live and improved live evaluation

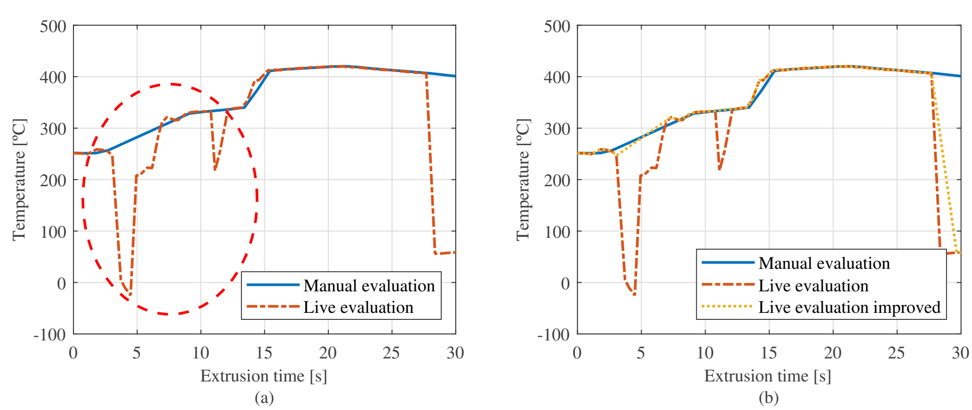

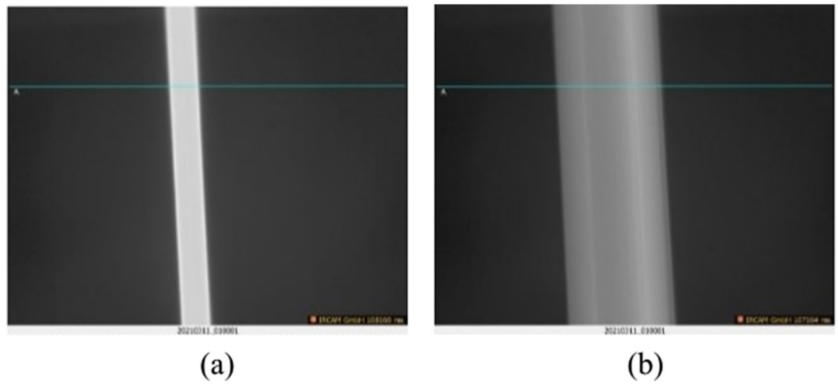

Fig. 4 Image from IRCAM (**a**) unfocused; **b** focused

studies starts from a high-speed value and exponentially decreases until almost stable speed. The required steady-state temperature and load define the maximum speed value to reach the desired temperature at the early stages [14, 16]. For instance, Li et al. [15] have set the starting speed at 8 mm s^{-1} and decreased it to 2 mm s^{-1} to extrude AZ31 at 400 °C. Based on this, in the case of the EMS, 1 mm s^{-1} was defined as the maximum and starting extrusion speed to obtain an extrusion temperature of 260 °C based on the results obtained in E05 (presented later).

Figure 5 shows the real-time response obtained for the bar temperature and the ram speed during the extrusion. Figure 5a illustrates the evolution of the reference and measured temperature during extrusion. It should be mentioned that an unexpected temperature peak is measured at around 40-60 s. This could be related to the particles on the surface of the extruded profile or the light emissivity according to the angle of the surface. To solve this issue, the high temperature values derived from the previously mentioned options should not be considered. For instance, in future works, the problem could be overcome during the temperature evaluation by excluding the points whose temperature value stands out from the average of the rod.

Figure 5b represents the evolution of the reference and measured speed. The measured speed appropriately follows the reference speed defined by the control lookup table. Nonetheless, between extrusion times 90-115 s and 135-165 s, the specified lookup table lead to continuous speed reference changes, generating speed oscillations. In Fig. 5c, the measured temperature and speed can be observed. The acquired speed response agrees with the temperature evolution. The extrusion is started with the maximum defined speed (1 mm s^{-1}). After a few seconds, the speed is reduced rapidly as a response to the obtained temperature, in good agreement with previous works [14–16]. Indeed, when a higher temperature is measured, the implemented speed control decreases the reference speed and vice versa. This is clearly represented at around extrusion time 40-60 s. Hence, it is concluded that the implemented live speed control system (described in Fig. 3c) could adequately control the extrusion press speed depending on the rod temperature measured by the IRCAM.

Despite the system and concept being validated, the used control algorithm based on a lookup table could be improved to have a better response of the speed. As previously mentioned, a lookup table is used because of its simplicity and facility for implementing the speed control algorithm. This lookup table is defined based on the temperature results obtained on E05 (presented later), where a final extrusion temperature of around 270 °C is received at a constant extrusion speed of 0.5 mm s^{-1}. Even so, if a higher extrusion temperature is required for the same initial temperature, the

Fig. 5 Automated extrusion process bar evolution of (**a**) reference and measured temperatures; **b** reference and measured ram speed; **c** measured temperature and speed

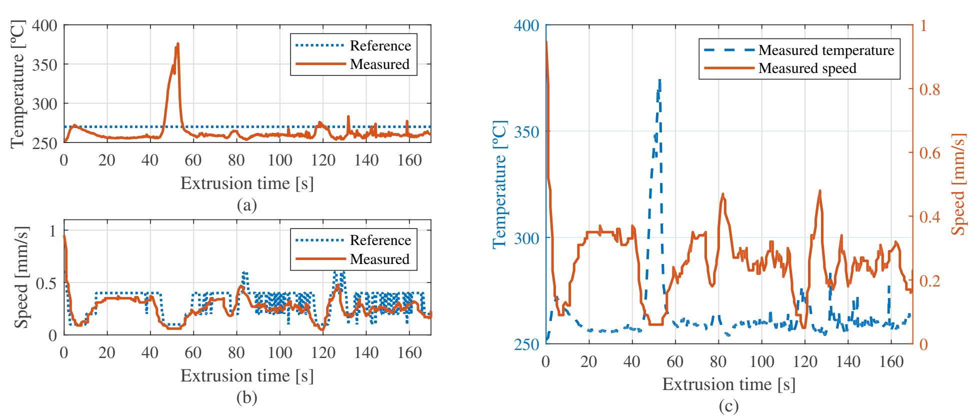

lookup table should be adjusted depending on the specific needs. Otherwise, the defined maximum speed could be insufficient to reach the desired temperature at the initial extrusion stage rapidly. This drawback could be improved by implementing an alternative control algorithm, such as the PID, which has been proven to offer good speed profiles to obtain isothermal extrusions [15, 16].

Extrusion temperature and pressure analysis

The pressure and temperature of the extrusions performed at 0.5 and 5 mm s^{-1} (E05 and E5, respectively) and multi-speed (EMS) are shown in Fig. 6. All extrusions show an initial increase and consecutive gradual decrease of the pressure during the extrusion, where EMS offer the minimalized pressure reduction. This trend curve is a typical pressure curve obtained during direct extrusion. It is observed that a higher initial pressure is developed in the extrusion with a higher speed compared to E5 and E05. The increase in extrusion speed influences the extrusion pressure, which is a consistent result of the previous work [14, 16, 17].

Figure 7 shows the comparison between the temperature evolutions obtained during the extrusion of the E5, E05, and EMS. In the E5 and E05, the temperature increase can be divided into two fractions [4]. Firstly, the die exit temperature rapidly increases at the beginning of the extrusion. When the billet material reaches the die and starts flowing, high local internal friction occurs, and the generated heat increases the temperature. This temperature increase is enhanced with speed. Secondly, as the extrusion proceeds, the heat generated due to deformation is transferred by thermal conductivity to the extruded profile and external environment, as well as to the extrusion tools and remaining billet. Therefore, the temperature increase in the second fraction is not as fast as the first one. Hence, a temperature gradient occurs from the beginning to the end of the extrusion due to the effects mentioned above [4, 14, 16]. In the case of the E5, the temperature increases

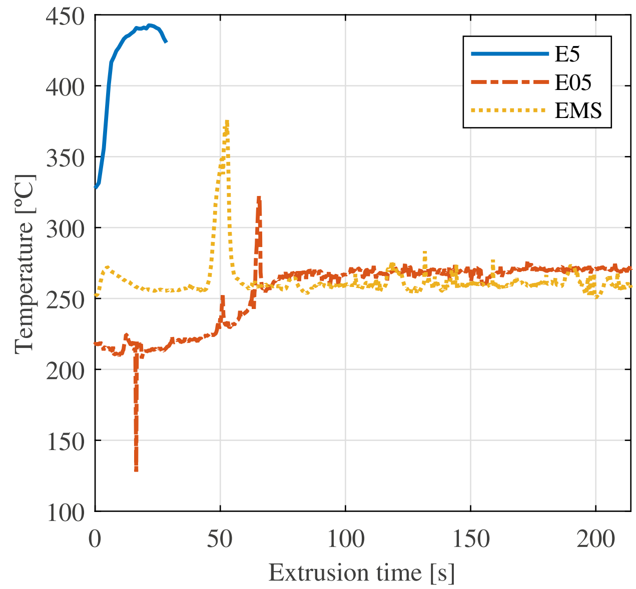

Fig. 7 Temperature evolution of the bar at fixed 5 (E5) and 0.5 (E05) mm s-1 speed and multi-speed control (EMS)

by approximately 100 °C from the beginning to the end of the extrusion, while the temperature rises about 50 °C in the E05. When high-speed extrusion is overcome, heat generation is mainly derived from the forehead-mentioned internal friction [4, 14, 16]. Due to the reduced conduction time, this heat is not released, resulting in a high-temperature gradient and a non-isothermal extrusion (Fig. 7 E5). Contrarily, when speed is reduced, the primary heat source is the material deformation, which is transferred by thermal conductivity. Therefore, temperature evolution is more stable and almost isothermal extrusion is conducted (Fig. 7 E05).

In the EMS (Fig. 7), an utterly isothermal temperature evolution is obtained with the controlled extrusion speed. As a result, the temperature gradient obtained in the extruded bar is 10 °C, without considering the peak temperature at

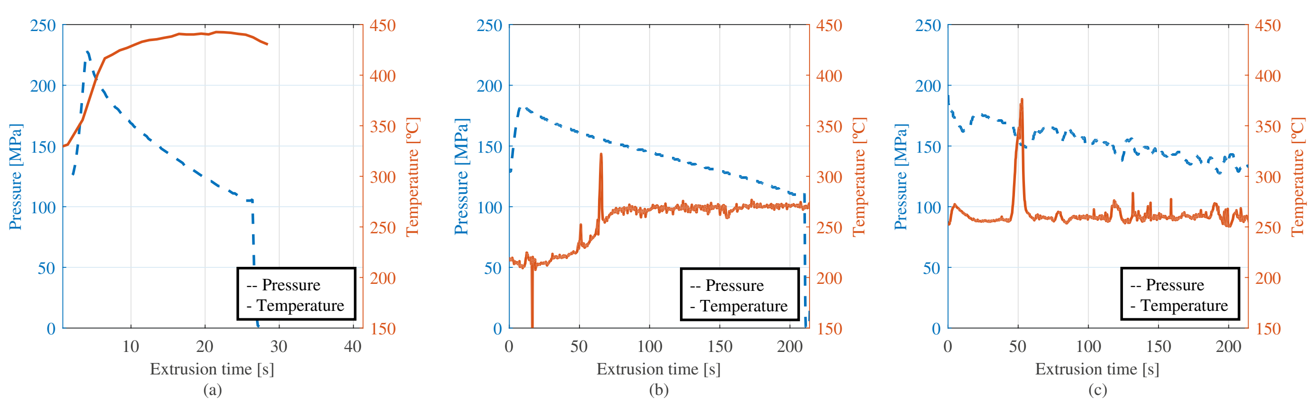

Fig. 6 Extrusion pressure and temperature evolution for (**a**) E5; **b** E05; **c** EMS

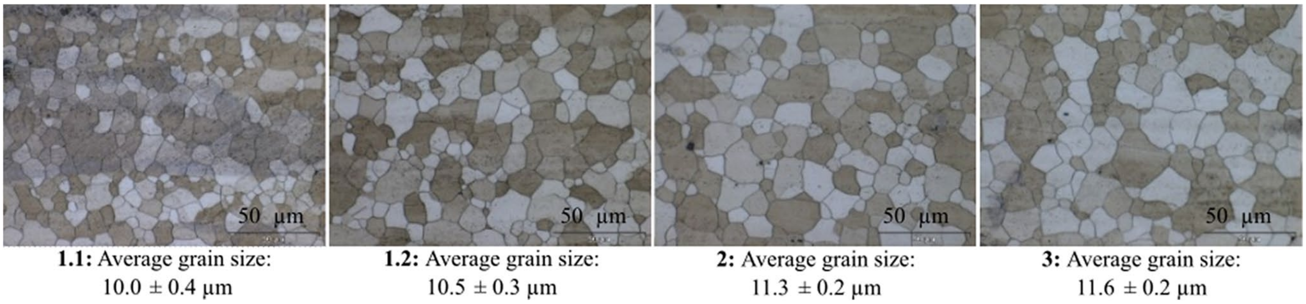

Fig. 8 Microstructure observed at the sample positions 1.1, 1.2, 2, and 3 of the extruded bar in the E5

50s. This is comparable to the results for the extrusions with predefined ram speed profiles in previous works [15, 16]. The stable temperature reached in EMS compared to E5 and E05 can benefit the homogeneous evolution of the microstructure.

Microstructure analysis

The microstructure of the E5 and E05 are shown in Figs. 8 and 9, respectively. In the E5, the microstructure shows the equiaxed grains. However, the grain size is slightly increased from 10.0 μm at the beginning (sample 1.1) to 11.6 μm at the ending (sample 3) positions during the extrusion. This grain growth is associated with the high temperature increase during the extrusion, which increases around 100 °C. A similar microstructure evolution has been reported in the work of Isakovic et al. [4]. It has also been observed that the AZ31 extruded bar at 300 °C with an extrusion speed of 6.7 mm s^{-1} presented a grain growth of 3 μm with a temperature gradient of 110 °C.

On the contrary, a relatively similar microstructure is observed in the whole extruded bar in the E05. The grain size difference during extrusion is slight, approximately 0.5 μm, due to the lower temperature difference from the slow extrusion speed. This suggests that the isothermal temperature evolution can result in a homogeneous microstructure, which is consistent with previous work results [4, 13]. A lower initial extrusion temperature due to a lower speed also influences the smaller grain size of the E05. Similar behavior of the microstructure has been seen by Elsayed et al. [18], Fan et al. [17] and Isakovic et al. [4], where it has been concluded that lower extrusion speed refined the grain size in extruded AZ31. Furthermore, in addition to the temperature increase, Zhou et al. [19] related a coarser and non-homogeneous microstructure with the incomplete DRX due to decreased deformation time for an extrusion speed of 1 mm s^{-1} compared to 0.1 mm s^{-1} (in curved AZ31 profile extrusion).

Considering the conclusions obtained from the microstructure analysis of the E5 and E05, a homogeneous microstructure evolution could be anticipated in the EMS due to its stable temperature evolution and slow extrusion speed profile. Compared to E5 and E05, a smaller grain size is obtained in EMS. In addition to the obtained lower extrusion temperature, this could be related to the longer deformation time derived from, the lower extrusion speed, as explained in [19]. However, there is a slight grain growing effect from 5.5 to 7.1 μm, as shown in Fig. 10. A stable temperature is obtained since the initial stage of the extrusion, which results in a negligible grain size difference (around 0.6 μm) between the samples 1.1, 1.2 and 2. The grain growth is mainly observed between samples 2 and 3, around 1 μm. This could be related to the speed and temperature evolution of the EMS at the end of the extrusion (Fig. 5). From the extrusion time of

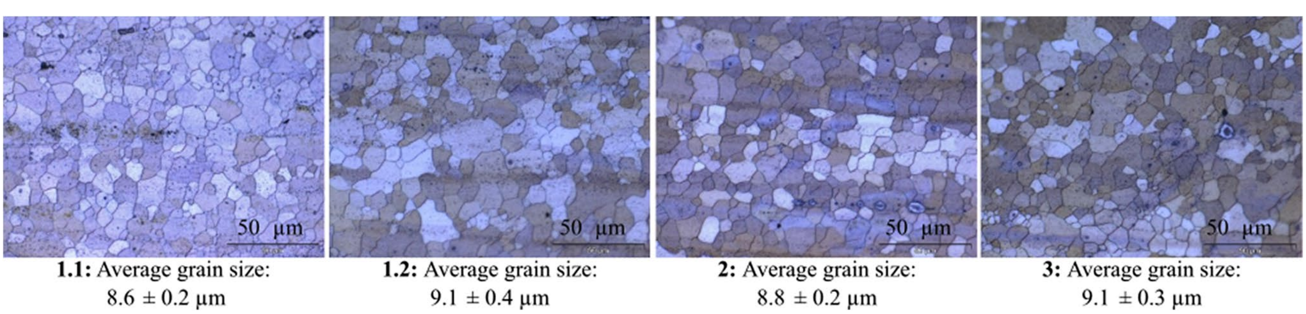

Fig. 9 Microstructure observed at the sample positions 1.1, 1.2, 2, and 3 of the extruded bar in the E05

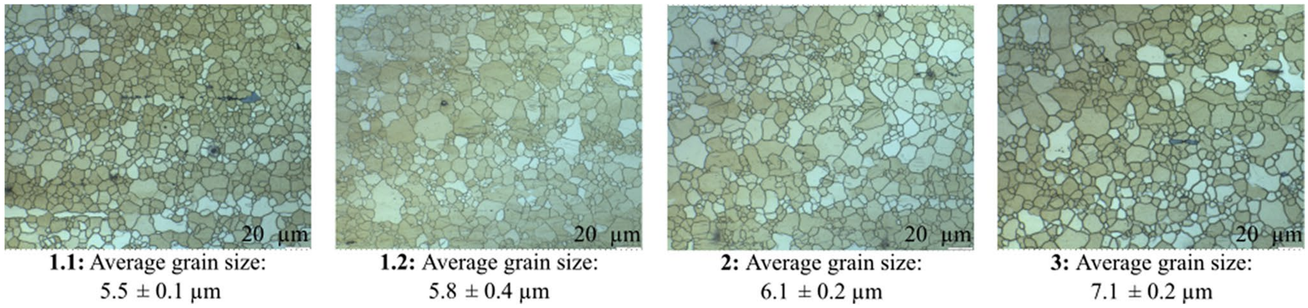

Fig. 10 Microstructure observed at the sample positions 1.1, 1.2, 2, and 3 of the extruded bar in the EMS

100 s on, which corresponds to the sample position 3, the speed is abruptly varied, and the temperature profile is not as smooth as the beginning of extrusion. Despite not having a fully homogenized microstructure yet obtained with the present speed control strategy, the speed variations could be smoothed by implementing a new control algorithm, such as PID. Nonetheless, using this type of algorithm requires further studies regarding microstructure homogeneity.

Conclusion

This study suggested an alternative method to control the microstructure development during the extrusion of AZ31 based on the control of extrusion speed and temperature in real-time. The system based on the speed control depending on the temperature measured by the IRCAM was successfully developed.

In constant speed extrusions at 5 and 0.5 mm s^{-1} (E5 and E05, respectively), the temperature was increased due to the internal friction during the extrusion. This was associated with the inhomogeneous microstructure development, especially observed in E5. On the contrary, the EMS showed a stable temperature and further relative homogeneous microstructure at the beginning of the extruded bar. In summary, the extrusion speed control in real-time effectively influenced the microstructure development with the stable temperature. Although the only data obtained from the speed control extrusion between 0.1 and 1 mm s^{-1} was shown in this study, the temperature and speed evaluation in real-time of the EMS showed the possibility of optimizing the extrusion process. For more accurate control, it is essential to improve the control algorithm, e.g., implementing PID control.

Acknowledgements The authors are grateful to Alexander Reichart at Helmholtz-Zentrum hereon for his technical support. The authors are grateful for financial support from the Helmholtz-Zentrum hereon (I2B-grant).

Author contribution Leire Elorza Azpiazu: Conceptualization, Investigation, Experimentation, Data processing, Writing-original draft, Reviewing and editing.

Aritz Egea: Supervision, Reviewing and editing.

Dietmar Letzig: Supervision, Reviewing and editing.

Changwan Ha: Supervision, Investigation, Experimentation, Reviewing and editing.

Funding Open Access funding enabled and organized by Projekt DEAL.

Declarations

Ethics approval The article fulfils the guidelines of the Committee on Publication Ethics (COPE) and involves no studies on human or animal subjects.

Consent to participate Not applicable.

Consent for publication Not applicable.

Conflicts of interest/Competing interests The authors declare that they have no conflicts of interest/competing interests relevant to the content of this article.

References

1. Yang Z et al (2008) Review on Research and Development of magnesium alloys. Acta Metallurgica Sinica (English Letters) 21(5):313–328. https://doi.org/10.1016/S1006-7191(08)60054-X
2. Avedesian M, Baker H (eds) (1999) Magnesium and magnesium alloys. ASM International
3. Guo L, Yang H (2014) Deformation rules and mechanism of large-scale profiles extrusion of difficult-to-deform materials.

Comprehensive Materials Processing Edited by H Saleem et al Elsevier doi. https://doi.org/10.1016/B978-0-08-096532-1.00524-0
4. Isakovic J et al (2022) Microstructure development of magnesium alloys AZ31 and AZ80 due to temperature evolution during direct extrusion. In Proceedings of the International Aluminum Extrusion Technology, Orlando, FL, USA
5. Zeng Z et al (2018) Magnesium extrusion alloys: a review of developments and prospects. Int Mater Rev. https://doi.org/10.1080/09506608.2017.1421439
6. Xu C et al (2017) Development of ultra-high strength and ductile mg–Gd–Y–Zn–Zr alloys by extrusion with forced air cooling. In: Minerals, metals and materials series. Springer International Publishing, pp 23–28. https://doi.org/10.1007/978-3-319-52392-7_7
7. Park SH et al (2015) Improved strength of mg alloy extruded at high speed with artificial cooling. J Alloys Compd 648:615–621. https://doi.org/10.1016/j.jallcom.2015.06.219
8. Park SH, Kim HS, You BS (2015) Improving the tensile strength of mg-7Sn-1Al-1Zn alloy through artificial cooling during extrusion. Mater Sci Eng A 625:369–373. https://doi.org/10.1016/j.msea.2014.12.011
9. Kim B et al (2013) Grain refinement and improved tensile properties of mg-3Al-1Zn alloy processed by low-temperature indirect extrusion. Scr Mater 76:21–24. https://doi.org/10.1016/j.scriptamat.2013.12.005
10. Hsiang SH, Kuo JL (2003) An investigation on the hot extrusion process of magnesium alloy sheet. J Mater Process Technol 140(1-3 SPEC):6–12. https://doi.org/10.1016/S0924-0136(03)00693-9
11. Zeng ZR et al (2018) Achieving exceptionally high strength in mg–3Al–1Zn-0.3Mn extrusions via suppressing intergranular deformation. Acta Mater 160(September):97–108. https://doi.org/10.1016/j.actamat.2018.08.045
12. Murai T et al (2003) Effects of extrusion conditions on microstructure and mechanical properties of AZ31B magnesium alloy extrusions. J Mater Process Technol 141(2):207–212. https://doi.org/10.1016/S0924-0136(02)01106-8
13. Chanda T, Zhou J, Duszczyk J (2001) A comparative study on iso-speed extrusion and isothermal extrusion of 6061 Al alloy using 3D FEM simulation. J Mater Process Technol 114(2):145–153. https://doi.org/10.1016/S0924-0136(01)00724-5
14. Zhou J, Li L, Duszczyk J (2004) Computer simulated and experimentally verified isothermal extrusion of 7075 aluminium through continuous ram speed variation. J Mater Process Technol 146(2):203–212. https://doi.org/10.1016/J.JMATPROTEC.2003.10.018
15. Li LX, Lou Y (2008) Ram speed profile design for isothermal extrusion of AZ31 magnesium alloy by using FEM simulation. Trans Nonferrous Metals Soc China 18(SPEC. ISSUE 1):s252–s256. https://doi.org/10.1016/S1003-6326(10)60212-9
16. Yi J, Liu ZW, Zeng WQ (2021) Isothermal extrusion speed curve design for porthole die of hollow aluminium profile based on PID algorithm and finite element simulations. Trans Nonferrous Metals Soc China 31(7):1939–1950. https://doi.org/10.1016/S1003-6326(21)65628-5
17. Fan X et al (2010) Effects of dynamic recrystallization in extruded and compressed AZ31 magnesium alloy. Acta Metallurgica Sinica (English Letters) 23(5):334–342. https://doi.org/10.11890/1006-7191-105-334
18. Elsayed FR et al (2013) Effect of extrusion conditions on microstructure and mechanical properties of microalloyed mg-Sn-Al-Zn alloys. Mater Sci Eng A 588:318–328. https://doi.org/10.1016/j.msea.2013.09.050
19. Zhou W, Lin J, Dean TA (2022) Microstructure and mechanical properties of curved AZ31 magnesium alloy profiles produced by differential velocity sideways extrusion. Journal of Magnesium and Alloys. https://doi.org/10.1016/j.jma.2022.11.012